

Communications

$K_8In_{10}Zn$: Interstitially-Stabilized Analogues of Early-Transition-Metal Halide Clusters

Slavi C. Sevov and John D. Corbett*

Ames Laboratory¹ and Department of Chemistry, Iowa State University, Ames, Iowa 50011

Received October 14, 1992

Convergence of the principles that afford both interstitially-stabilized halide clusters of the early transition metals and hypoelectronic clusters of main-group elements has been realized in the centered clusters present in the new compound $K_8(In_{10}Zn)$. Zintl or "naked" clusters of the post transition elements (Sn_9^{4-} , Pb_5^{2-} , Bi_4^{2-} , etc.) generally follow Wade's rules and therefore contain a minimum of $2n + 2$ skeletal bonding electrons in p-orbital-based MO's.² Although analogous ions for members of the aluminum family are unknown, perhaps because of the requisite high charges, i.e., $closo-M_n^{(n+2)-}$, a hypoelectronic ($2n - 4 e^-$) example In_{11}^{7-} (D_{3h}) in $K_8In_{11}^3$ and the closely related substituted cluster in $K_8In_{10}Hg^4$ were recently discovered. In these instances, fortuitous electronic consequences of both polyhedral capping and distortion allow access to this new cluster regime. Several other nearly-electron-precise compounds with structures consisting of interconnected clusters, both familiar and new, further attest to the strength and dominance of In-In⁴⁻⁶ (and Ga-Ga⁷⁻⁹) bonding. At the other extreme, a large family of nominally electron-poor, octahedral M_6X_{12} -type clusters of the group 3 and 4 transition metals have been synthesized in which one of a diverse list of atoms centered within each cluster is necessary for thermodynamic stability.¹⁰⁻¹² Centered indium cluster ions have now been discovered in which exactly the same effects are operative, namely, the provision of additional electrons and central bonding by the interstitial. This paper reports on the first example, $In_{10}Zn^{8-}$, which is nominally D_{4d} and has $2n = 20$ skeletal bonding electrons.

Fusion of the elements in the indicated proportions at 600 °C in a welded Ta container followed by slow cooling (3 °C/h) affords

a single-phase sample of $K_8In_{10}Zn$ according to a comparison of the Guinier powder photograph of the product with that calculated on the basis of the refined structural parameters. The compound is very brittle and dark with a slight yellow luster. Analogous products are not obtained with Na, Rb, Cs, Cd, or Hg.

Single-crystal studies¹³ reveal the presence of discrete bicapped Archimedean antiprisms of indium, the classic polyhedron for a *closo*- M_{10} unit, but these are both distorted and centered by a zinc atom (Figure 1). The clusters have 422 (D_4) symmetry with In₂ and Zn lying on the 4-fold axis. The deviations from D_{4d} correspond to only a 1.73° torsional twist of the opposed squares and a 0.092-Å difference in the In1-In1 distances, which we presume arise from packing effects. The skeletal distortions serve to put the zinc atom nearly equidistant from all members of the indium shell. This means the edges of the square faces of the antiprism are 0.57 Å longer than the average of the In-In separations marked by solid lines, 3.072 Å. The last is close to the average in In_{11}^{7-} , 3.090 Å,^{3,14} indicating the presence of both comparable bonding within the indium shell and an interstitial prop that is of appropriate size. We are unable to find In-Zn distances in any other compound with which to compare the observed 2.836-Å average, but the uncritical use of the sum of Pauling's single-bond metallic radii¹⁵ for the two metals (2.634 Å) gives an average bond order of 0.46, not unreasonable in view of the electronic structure (below).

There is only one type of potassium in the structure, and this appears to have fairly specific interactions with the cluster anions, as generally observed. Each cation has three cluster neighbors on which it caps a triangular face of In1 atoms about the waist of one (at 3.56-3.96 Å), bridges an In1-In2 edge in a second (3.77 Å), and is exo to a single In1 in a third (3.76 Å). This arrangement in effect means that In2 vertices in the staggered square layers of clusters penetrate the double potassium layers that lie between these layers (see frontispiece), in contrast to the

- (1) Ames Laboratory is operated for the Department of Energy by Iowa State University under Contract No. W-7405-Eng-82. This research was supported by the U.S. Department of Energy, Office of Basic Energy Sciences, Materials Sciences Division.
- (2) Corbett, J. D. *Chem. Rev.* **1985**, *85*, 383.
- (3) Sevov, S. C.; Corbett, J. D. *Inorg. Chem.* **1991**, *30*, 4875.
- (4) Sevov, S. C.; Corbett, J. D. Unpublished research.
- (5) Sevov, S. C.; Corbett, J. D. *Inorg. Chem.* **1992**, *31*, 1895.
- (6) Sevov, S. C.; Corbett, J. D. *J. Solid State Chem.*, in press.
- (7) Belin, C.; Tillard-Charbonnel, M. *Prog. Solid State Chem.* **1993**, *22*, 59.
- (8) Schäfer, H. J. *Solid State Chem.* **1987**, *57*, 210.
- (9) Burdett, J. K.; Canadell, E. J. *Am. Chem. Soc.* **1990**, *112*, 7207.
- (10) Ziebarth, R. P.; Corbett, J. D. *Acc. Chem. Res.* **1989**, *22*, 256.
- (11) Zhang, J.; Corbett, J. D. *Inorg. Chem.* **1991**, *30*, 437.
- (12) Corbett, J. D. In *Modern Perspectives in Inorganic Crystal Chemistry*; Parthé, E., Ed.; NATO ASI Series C; Kluwer Academic Publishers: Dordrecht, The Netherlands, 1992; p 27.

- (13) The structure was solved by direct methods (SHELX-86) following data collection at 22 °C on a CAD 4 diffractometer with Mo K α radiation. Crystal data: $P4/nnc$ (No. 126), $Z = 2$; $a = 10.2916(5)$ Å, $c = 13.837(1)$ Å (from Guinier data, $\lambda = 1.54056$ Å), $R/R_w = 2.1\%/2.1\%$ for 427 independent reflections ($2\theta \leq 50^\circ$) and 25 variables after absorption correction ($\mu = 95.5 \text{ cm}^{-1}$) with the aid of the average of two ψ scans. The largest density in the difference Fourier map, $0.66 \text{ e}/\text{Å}^3$, was 1.3 Å from K. The F_o , F_c data are available from J.D.C.
- (14) The longer but still relevant $d(\text{In1-In1})$, 3.627(2) Å, was missing from the previous listing for In_{11}^{7-} .
- (15) Pauling, L. *The Nature of the Chemical Bond*; Cornell University Press: Ithaca, NY, 1960; p 400.

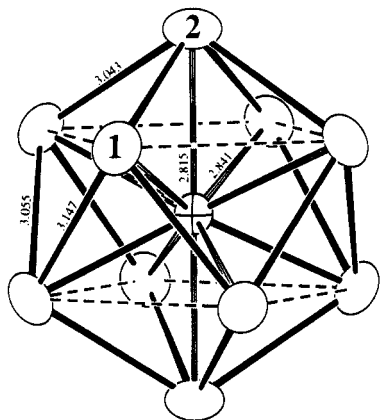


Figure 1. The cluster anion $\text{In}_{10}\text{Zn}^{8-}$. The cluster has D_{4d} symmetry, and its principal axis is vertical. (Thermal ellipsoids at the 94% probability level.)

greater separation of the less symmetric clusters that lie between double cation layers along \bar{c} in K_8In_{11} .³ The shortest K–K and intercluster In–In separations here are 4.26 and 5.58 Å, 0.2 and 0.3 Å greater, respectively, than in the metallic K_8In_{11} .

The electronic consequences of this composition and structure are readily appreciated with the results of extended Hückel calculations.¹⁶ Figure 2 shows these for the dominantly p-orbital states (a) in the classic bicapped square antiprism (with the same average edge lengths as in $\text{In}_{10}\text{Zn}^{8-}$), (b) after the observed lateral expansion and axial compression necessary to make all vertices substantially equidistant (2.84 Å) from the centroid, and (c) following encapsulation of the zinc atom in the distorted polyhedron.¹⁷ The distortion from (a) to (b) raises the penultimate a_1 to a future LUMO role in (c) through expansion of the square faces of the antiprism where this MO is both σ - and π -bonding via p_z . Interactions of the other three high-lying bonding orbitals a_1 , e_1 , and b_2 in the distorted cluster (b) with the s , $p_x p_y$, and p_z valence orbitals, respectively, of the inserted Zn obviously stabilize this hypothetical intermediate (c). Each of the three involves a three-level MO system. The lowest lying a_1 (–9.05 eV) in the centered cluster contains Zn s and predominantly In s , while the bonding a_1 near –5.0 eV is largely Zn s mixed with In s and p . A low-lying e_1 (not shown) contains mainly In s with a little In p , but negligible Zn p , while the two e_1 's shown are made up of In p plus Zn $p_x p_y$, the latter making a somewhat greater contribution to the bonding level. The energy distribution of these two is in accord with the relative large overlap integral. Three relevant b_2 levels are present. The upper two b_2 levels shown in (c) involve mainly s and p_z orbitals on the axial In2 atoms, again with proportions as with e_1 , while the low-lying b_2 (–7.70 eV) has some Zn p_z mixed in. This last set is presumably responsible for the somewhat shorter In2–Zn axial distance.

The results are quite consistent with the observed closo but centered cluster with 20 skeletal electrons [$8(\text{K}) + 10(\text{In } p) + 2(\text{Zn})$]. This contrasts with the ideal but unknown empty cluster In_{10}^{12-} that would have $2n + 2 = 22$ electrons and a charge greater by 4, i.e., with a_1 as the HOMO in Figure 2a. The difference of 4 comes equally from the distortion and the two electrons contributed by zinc.

The role of the interstitial zinc is strikingly similar to that in many other electron-poor M_6X_{12} -type clusters of zirconium,

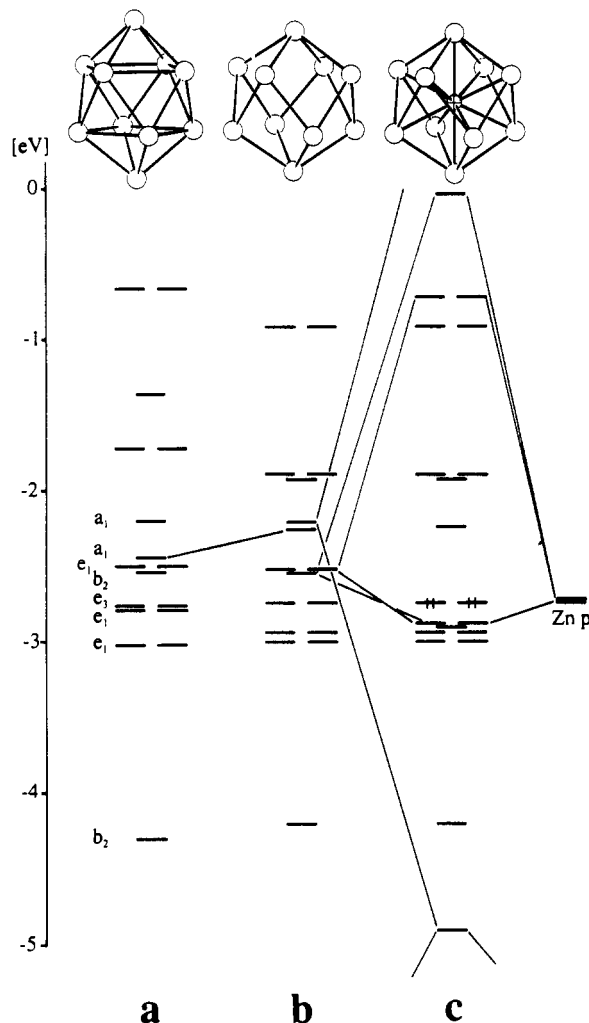


Figure 2. Charge-consistent extended-Hückel MO results for hypothetical In_{10} precursors and for $\text{In}_{10}\text{Zn}^{8-}$ (D_{4d}): (a) for the classical 10-atom polyhedron; (b) after distortion to the observed shell dimensions; (c) after zinc insertion. The $b_2(2)$ level near –4.3 eV contains both In $5s$ and $5p$ contributions and lies at the top of the s -based orbitals (not shown).

hafnium, and the rare-earth metals where encapsulation of a main-group (or transition-metal) element likewise affords an essential stabilization through additional electrons and central bonding but no new bonding orbitals.^{10,12} (As in $\text{In}_{10}\text{Zn}^{8-}$, certain skeletal bonding orbitals in the empty transition-metal cluster have the same representations as s and p (or d) on the interstitials, and the corresponding pairs of more bonding and high-lying antibonding levels are produced in the encapsulation process.) Examples are $\text{Sc}(\text{Sc}_6\text{Cl}_{12}\text{N})$, $\text{Zr}_6\text{Cl}_{12}\text{Be}$, and $\text{Zr}_6\text{I}_{14}\text{C}$, all with $2n + 2 = 14$ bonding electrons, counting those of the interstitial as well. These and the $\text{In}_{10}\text{Zn}^{8-}$ examples are all stable in a thermodynamic sense, that is, with respect to all alternate products. Ordinary chemistry does not afford much guidance for prognostication of other cluster examples, but several other apparent interstitial or substitution derivatives of indium clusters are presently under study. One tantalizing series is the isostructural $\text{K}_{10}\text{In}_{10}\text{M}$ ($\text{M} = \text{Ni}, \text{Pd}, \text{Pt}$), in which the d orbitals on Ni etc. are effectively corelike and nonbonding and valence s and p orbitals are responsible for the bonding. The nickel-centered polyhedron is closest to C_{3v} symmetry, but it is in fact also a recognizable distortion of the $\sim D_{4d}$ polyhedron of $\text{In}_{10}\text{Zn}^{8-}$.⁴ It is interesting to note that In_{11}^{7-} is also isoelectronic with both $\text{In}_{10}\text{Zn}^{8-}$ and $\text{In}_{10}\text{Ni}^{10-}$, one skeletal atom in the first being converted to the role of a smaller interstitial in the other two.

The magnetic susceptibility data for $\text{K}_8\text{In}_{10}\text{Zn}$ from SQUID measurements are shown in Figure 3 after correction for the special container⁵ as well as for core (-3.04×10^{-4} emu mol⁻¹)

(16) The orbital exponents used for In were as before³ while those for Zn were taken from: Janiac, C.; Hoffman, R. *J. Am. Chem. Soc.* **1990**, *112*, 5924. The H_{ij} values for both were iterated to charge consistency (Zn $4s = -6.14$, $4p = -2.72$ eV; In $5s = -6.47$, $5p = -2.40$ eV) with the aid of parameters given by: Munita, R.; Letelier, J. R. *Theor. Chim. Acta* **1981**, *58*, 167. The same H_{ij} values for In were used for the In_{10} clusters shown in Figure 2.

(17) The b_2 level near –4.3 eV exhibits significant hybridization of s and p , but the AO signs on the antiprismatic atoms are out of phase with a central p_z orbital and so this level remains unchanged across the series.

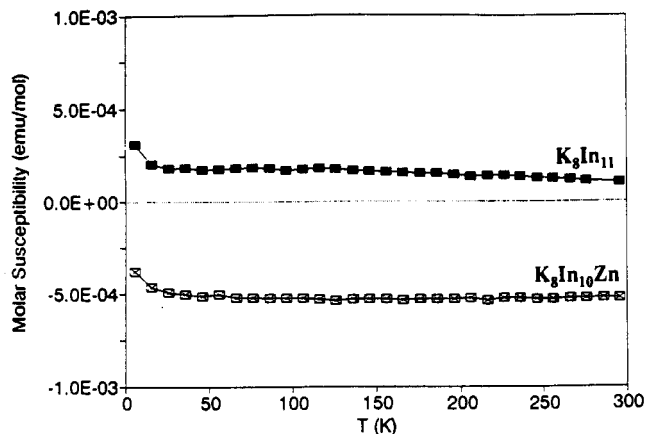


Figure 3. Molar magnetic susceptibility data for $K_8In_{10}Zn$ relative to those for the metallic K_8In_{11} .³ Both have been corrected for core and orbital (Langevin) diamagnetic contributions.

and cluster orbital or Langevin ($-3.23 \times 10^{-4} \text{ emu mol}^{-1}$) effects, as before.^{3,6} Shown for comparison are the data for the metallic and similarly corrected $(K^+)_8In_{11}^{7-e^-}$. The additional electronic localization in the zinc compound is clear. On the other hand, electrodeless "Q" measurements indicate a metal-like conductivity for $K_8In_{10}Zn$, with $\rho_{295} \sim 260 \mu\Omega \text{ cm}$ and a coefficient of 0.32% per degree over the range 140–295 K. Such seemingly conflicting properties have been repeatedly observed for other salts containing what are predicted to be closed-shell clusters of main-group metals, viz., $In_{10}Hg^{8-}$, In_4^{8-} , and Sn_4^{4-} .^{4,6,18} Although no specific studies have addressed these problems, some general observations suggest some reasonable interpretations. Many main-group metals themselves are similarly disposed, indium itself having $\rho_{293} \sim 8.4 \mu\Omega \text{ cm}$, but $\chi_M(293) = -45 \times 10^{-6} \text{ emu mol}^{-1}$ after core correction.²⁰ Categorical interpretations of these involve the effects of large overlap and wide bands and thence low densities

of states at E_F , which in turn result in smaller effective masses for the conduction electrons. The last correlate, on one hand, with low Pauli paramagnetic but high Landau diamagnetic contributions to the susceptibility and, on the other, with higher charge mobilities that emphasize the electronic conduction.²¹ According to these ideas, the true "zero" in Figure 3 would presumably lie appreciably lower, by roughly $-60 \times 10^{-6} \text{ emu/mol}$ of In, comparable to the value for the metal.

The observed, relatively poor electronic conduction of course reflects what goes near the top of the valence band, where there is presumably some overlap with the conduction band. Such a result is not unreasonable in densely packed solids containing anions of a metallic main-group element like indium since this reduction will raise the atomic valence energies. Contributions of cation orbitals to the valence bands and of cluster antibonding MO's to the conduction band in these phases may be general and appreciable (as in Na_4Sn_4), but this cannot be handled in simple Hückel calculations. However, conduction via high-lying and substantially nonbonding levels should not obscure or lessen the obvious importance of localization in strong covalent In–In (or other) cluster bonds in lower lying valence levels/bands. The value and import of the descriptor "metallic Zintl phase"²² in these situations are clear.

Supplementary Material Available: Tables of data collection and refinement information, atom parameters, and distances and angles for $K_8In_{10}Zn$ (4 pages). Ordering information is given on any current masthead page.

- (18) The indicated charges are likely excessive. They better reflect conventional oxidation-state assignments but neglect probable charge delocalization through involvement of the cations in the bonding states, as demonstrated for Na_4Sn_4 .¹⁹
- (19) Springelkamp, F.; De Groot, R. A.; Geertsma, W.; van der Lugt, W.; Mueller, F. M. *Phys. Rev. B* **1985**, *32*, 2319.
- (20) *CRC Handbook of Chemistry and Physics*, 65th ed.; CRC Press: Boca Raton, FL, 1984; pp E-108, F-120.
- (21) Kittel, C. *Introduction to Solid State Physics*, 2nd ed.; J. Wiley: New York, 1956; p 293.
- (22) Nesper, R. *Prog. Solid State Chem.* **1990**, *20*, 1.